scientific reports

Check for updates

OPEN

Molecular dynamics and experimental analysis of energy behavior during stress relaxation in magnetorheological elastomers

Nurul Hakimah Lazim[1], Mohd Aidy Faizal Johari[1], Saiful Amri Mazlan[1,2]✉, Nur Azmah Nordin[1], Shahir Mohd Yusuf[1] & Michal Sedlacik[3,4]✉

The diverse applications of magnetorheological elastomer (MRE) drive efforts to understand consistent performance and resistance to failure. Stress relaxation can lead to molecular chain deterioration, degradation in stiffness and rheological properties, and ultimately affect the life cycle of MRE. However, quantifying the energy and molecular dynamics during stress relaxation is challenging due to the difficulty of obtaining atomic-level insights experimentally. This study employs molecular dynamics (MD) simulation to elucidate the stress relaxation in MRE during constant strain. Magnetorheological elastomer models incorporating silicone rubber filled with varying magnetic iron particles (50–80 wt%) were constructed. Experimental results from an oscillatory shear rheometer showed the linear viscoelastic region of MRE to be within 0.001–0.01% strain. The simulation results indicated that stress relaxation has occurred, with stored energies decreased by 8.63–52.7% in all MRE models. Monitoring changes in energy components, the highest final stored energy (12,045 kJ) of the MRE model with 80 wt% Fe particles was primarily attributed to stronger intramolecular and intermolecular interactions, revealed by higher potential energy (3262 kJ) and van der Waals energy (– 2717.29 kJ). Stress relaxation also altered the molecular dynamics of this MRE model as evidenced by a decrease in kinetic energy (9362 kJ) and mean square displacement value (20,318 Å^2). The MD simulation provides a promising quantitative tool for elucidating stress relaxation, preventing material failure and offering insights for the design of MRE in the nanotechnology industry.

Keywords Energy, Magnetorheological elastomer, Molecular dynamics simulation, Stress relaxation

Magnetorheological elastomer (MRE) has been widely used in various applications, including energy absorption, shock absorption, and vibration isolation systems for building and bridges, owing to tunable rheological properties when subjected to an external magnetic field. Generally, MRE exhibit the linear viscoelastic (LVE) region that represents an initial reversible deformation range where the molecular chains undergo insignificant rearrangement and can spontaneously return to their original form[1]. In addition, during LVE region, MRE could store elastic energy and resist deformation up to certain limit[2]. However, it is important to note that unlike purely elastic materials, MRE also exhibit viscous behavior. This means that over time, MRE can undergo time-dependent deformation and causes a gradual decline in properties of MRE. The time-dependent deformation in materials is often related to stress relaxation and fatigue phenomena. Fatigue refers to the progressive and localized structural damage that occurs when a material is subjected to cyclic loading or repeated stress over time[3], while stress relaxation refers to the gradual decrease in stress in a material subjected to a constant strain over time[4]. The stress relaxation in MRE has raised concerns because it could lead to the deterioration in molecular

[1]Engineering Materials and Structures (eMast) iKohza, Malaysia-Japan International Institute of Technology (MJIIT), Universiti Teknologi Malaysia, Jalan Sultan Yahya Petra, 54100 Kuala Lumpur, Malaysia. [2]Department of Mechanical Engineering, College of Engineering, University of Business and Technology (UBT), P.O. Box No. 21448, Jeddah, Saudi Arabia. [3]Department of Production Engineering, Faculty of Technology, Tomas Bata University in Zlín, 760 01 Zlín, Czech Republic. [4]Centre of Polymer Systems, University Institute, Tomas Bata University in Zlín, 760 01 Zlín, Czech Republic. ✉email: amri.kl@utm.my; msedlacik@utb.cz

chains and crosslink structures over a period of service. Additionally, stress relaxation can have significant implications for mechanical behavior of materials and may affect their structural integrity and performance in MRE. Consequently, this type of micro-deformation may limit the application of MRE to be used as flexible materials in energy and nanotechnology industries.

Johari et al.[5] has evaluated the durability performance of MRE using oscillatory shear rheometer for a total of 6010 s under constant strain of 0.01%. The study discovered that the storage modulus of MRE decreased by 0.5% by the end of test duration, indicating a stress relaxation phenomenon. Johari et al.[6] also utilized an oscillatory shear test for a duration of 84,000 s on MRE and reported the stress relaxation has developed strain localization and produced microplasticity in the shear band. Consequently, the shear stress, storage modulus and normal force of tested MRE decreased over this time of period. Study of stress relaxation phenomenon could provide insights about the durability performance for MRE to be used in long-term applications such as gaskets, seals, dampers and actuators[7]. Besides the experimental approach, another recent study by Nam and coworkers[8] presented both experimental and numerical simulations of isotropic and anisotropic MREs over 10 h using a single relaxation test. The work revealed that the shear stress and relaxation modulus under a strong magnetic field declined considerably after 0.25 h of testing. In a previous study, Nam et al.[9] also conducted single and multi-step relaxation tests using isotropic MREs for 1 h and found that the shear stress and relaxation modulus of MRE samples decreased over time, even at different constant strain levels of 0.05%, 0.10%, and 0.20%. Both studies discovered that the studied viscoelastic model fits well with the experimental data of the MRE. Despite these previous experimental and numerical modeling studies on the stress relaxation of MREs, detailed quantification of energy and dynamic motion of MREs during shear deformation at the atomic level needs further investigation. Furthermore, to the authors' knowledge, the study of the behavior of MREs subjected to constant strain over small-time scales within picoseconds is still limited. Therefore, conducting stress relaxation studies under small time scales is necessary to depict the changes in energy and rheological behavior of MREs and to avoid the failure of MREs when constant strain is applied.

In the present scenario of advanced computational technology, molecular dynamics (MD) simulation has attracted interest since it offers an "in silico first" approach to optimize the performance of materials in a relatively low-cost environment prior to experimental testing. The MD simulation is also accelerate the innovation process with the capability to predict the properties of modelled elastomers[10,11]. In fact, it complements laboratory experimentation with powerful materials informatics such as the glass transition temperatures[12], mechanical properties[13], thermodynamics[14] and other physical properties[15,16]. From previous studies, using atomistic MD simulation to predict various properties of materials is reliable and simulation results can be used to guide real material design[12]. When performing MD simulation, the choice of ensemble is important to accurately predict and analyze the properties of materials, especially when involving large particles in a modelled system. The ensemble is distinguished by which the variables are held constant throughout the simulation period[17]. For instance, Zhang et al.[18] introduced the NPT (constant number of particles (N), pressure (P), temperature (T)) ensemble through stepwise deformation and relaxation methods, by means of keeping the tensile velocity constant to allow sufficient relaxation in the crosslinked styrene-butadiene rubber model. The study discovered that the integration of both relaxation methods has improved the computational capability when the simulated engineering stress of the model has exceeded one order of magnitude than experimental results. For the shear deformation mode, in a recent study, Ji et al.[19] employed the NVT (constant number of particles (N), volume (V), temperature (T)) ensemble at 600 K with time steps of 50,000 and showed the simulated polymethylmethacrylate filled with silica stored non-bond energy mainly the van der Waals forces of about 95%. Jeong et al.[20] studied the stress relaxation in linear polyethylene and revealed the rheological properties decreased as the overall deformed chain structure become largely relaxed. Another study by Tamir et al.[21] predicted the relaxation modulus of fluoroelastomer using MD simulation and found the relaxation modulus is higher than experimental value. Despite the effort that has been made, the shear mode of the MD simulation in exploring the stress relaxation phenomenon of MRE from the atomic-level perspective is not well-exposed.

This work utilizes the MD simulation method as an additional characterization tool to investigate the energy and molecular dynamics behavior of MRE during the stress relaxation phenomenon. By using the NPT cell ensemble, the basic molecular characteristics behind the stress relaxation phenomena, particularly full energy forms such as stored, potential, and kinetic energies were quantified. The MRE models containing varying magnetic iron particles contents (50–80 wt%) were constructed and energy values were measured. The covalent and non-covalent bond interactions were also quantified. Moreover, the dynamics of the MRE based on radius of gyration and mean square displacement were also explored. The mechanism of stress relaxation based on illustration of particles displacement was studied using the dynamics analysis.

Results and discussion

Determination of linear viscoelastic region of MRE from oscillatory shear rheometry

The strain sweep via oscillatory shear rheometry test was performed to determine the LVE region of MRE. The test was repeated three times to ensure accuracy on MRE samples with 70 and 80 wt% of CIPs. Figure 1 represents a plot of storage modulus (*G'*) as a function of test duration for MRE samples with 70 and 80 wt% CIPs. Using time as the x-axis in Fig. 1 enhances the comprehension of MRE behavior over varying time scales, allowing for comparisons between simulation results and experimental data. This approach is particularly relevant as molecular dynamics (MD) simulations typically produce time series data used to derive properties such as energy. As the shear strain was increased continously from 0.001 to 10%, apparently, the LVE region is present within the strain of 0.001–0.01% in all three samples of MRE with 70 wt% CIPs. During the LVE region, an average *G'* of 327 kPa was observed for the MRE with 70 wt% CIPs–1,2, and 3 samples. The similar LVE region are also obtained in previous studies[6,22], and this indicates that molecular structure of MREs remains unchanged when

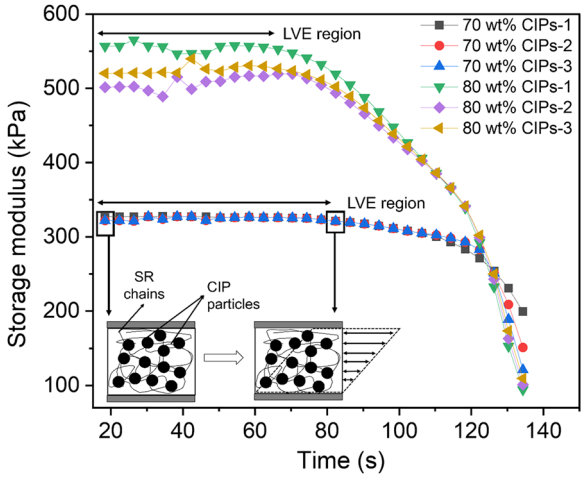

Fig. 1. Oscillatory shear rheometry test showing a linear viscoelastic region of MRE samples with 70 and 80 wt% CIPs.

this range of strain is applied, as illustrated in the Fig. 1. Meanwhile, MRE with 80 wt% of CIPs demonstrate shorter LVE region with higher *G'* ranges from 500 to 552 kPa than MRE with 70 wt% CIPs. This indicates that MRE with 70 wt% of CIPs are able to store energy for longer time than MRE with 80 wt% of CIPs. During the LVE region, the samples did not experience permenant deformation. However, after 80 s, the *G'* values of MRE began to decrease and finally reached values in the range of 120–199 kPa at final test duration of 134 s, indicating that the energy was starting to dissipate and leads to the breakdown of the MRE molecular chains.

Energy analysis of MRE under stress relaxation through MD simulation

After determination of the LVE region for MRE through experimental method, atomistic MRE models are simulated to a shear process within LVE region (fixed strain of 0.01%) using the MD simulation method. The MRE models are sheared for a total simulation time of 100 ps with 100,000 steps, and their stored energies (E_{stored}) are calculated. The E_{stored} can be a good evaluation for the ability of MRE in storing energy that propotionate to the storage modulus, which is one of the rheological properties. In addition, the measurement of E_{stored} provides information about the molecular bond interaction of MRE system from atomistic level. Utilizing time as the x-axis in Figs. 2 and 3 aids in pinpointing critical stages throughout the simulation and enhances the clarity of interpreting stress relaxation phases. The computed E_{stored} of MRE models 1, 2, 3, and 4 with various Fe contents of 50, 60, 70 and 80 wt%, respectively versus simulation time is plotted and shown in Fig. 2. When the strain of 0.01% is held constant for overall simulation time of 100 ps, it is apparent from Fig. 2a that the E_{stored} of all MRE models were gradually decreased over time MRE, signifies the strong indication to the stress relaxation phenomenon. Interestingly, the trend of the E_{stored} graph of MRE models is similar to the stress relaxation curve obtained from experimental testing[23] and mathematical modelling[24].

Based on the trend of the E_{stored} plot, the stress relaxation phenomenon in MRE can be divided into three main stages, namely the rapid stress relaxation (stage 1), stabilization and deformation (stage 2) and stable deformation stage (stage 3). During stage 1, the E_{stored} of MRE models decreases rapidly from the initial E_{stored}. This rapid stress relaxation stage is completed within approximately 0.3 ps in all models from the beginning of simulation time. This stage is also found in other previous studies[25,26]. It is also noticeable that the initial E_{stored} of MRE is higher when more Fe particles are added into SR, with the highest initial E_{stored} (25,289 kJ) for the MRE model 4. Although the simulated MRE model with 80 wt% Fe particles causes a relatively high initial E_{stored}, this model exhibits a high relaxation decrease in E_{stored} (32%) to 17,000 kJ by the end of stage 1, indicating a low ability to store energy within this time range. The similar finding is observed in previous rheological test that revealed 80 wt% CIPs have high storage modulus but it is a brittle sample because the presence of short LVE region[22]. It was also previously reported that increasing SiO_2 loading in natural rubber causes a substantial decrease in stress relaxation due to the more SiO_2 leads to progressive breakdown of the filler aggregates and causes the polymer chains get desorbed from the filler surface[27].

After the rapid stress relaxation stage, MRE models enters the stabilization and deformation stage as simulation time elapses after 0.3 ps. This region is called stabilization and deformation because the molecules in MRE model experience a steady-state increase in E_{stored} until the simulation time reaches 3 ps and followed by particles deformation by the half of simulation time of stage 2 (red dotted box (b)). The deformation stage starts approximately after 10% of the total simulation time. During stage 2, the E_{stored} pattern suggests that after rapid stress relaxation, the particles stabilizes to achieve stable deformation stage. In previous study, this is called physical relaxation mechanism that involves the rearranging of molecular chains towards new configuration in equilibirium at the new strained state[23]. It is noteworthy the higher onset deformation is observed with increasing Fe particles, for example model 4 deforms slower than model 2 (Fig. 2b). Previous study[28] found that 70 wt% of CIPs has increased the storage modulus in silicone rubber matrix than 60 wt% of CIPs. Hence, stiffer MRE needs longer time to deform and eventually increases onset deformation. Furthermore, beyond 60 ps of the total

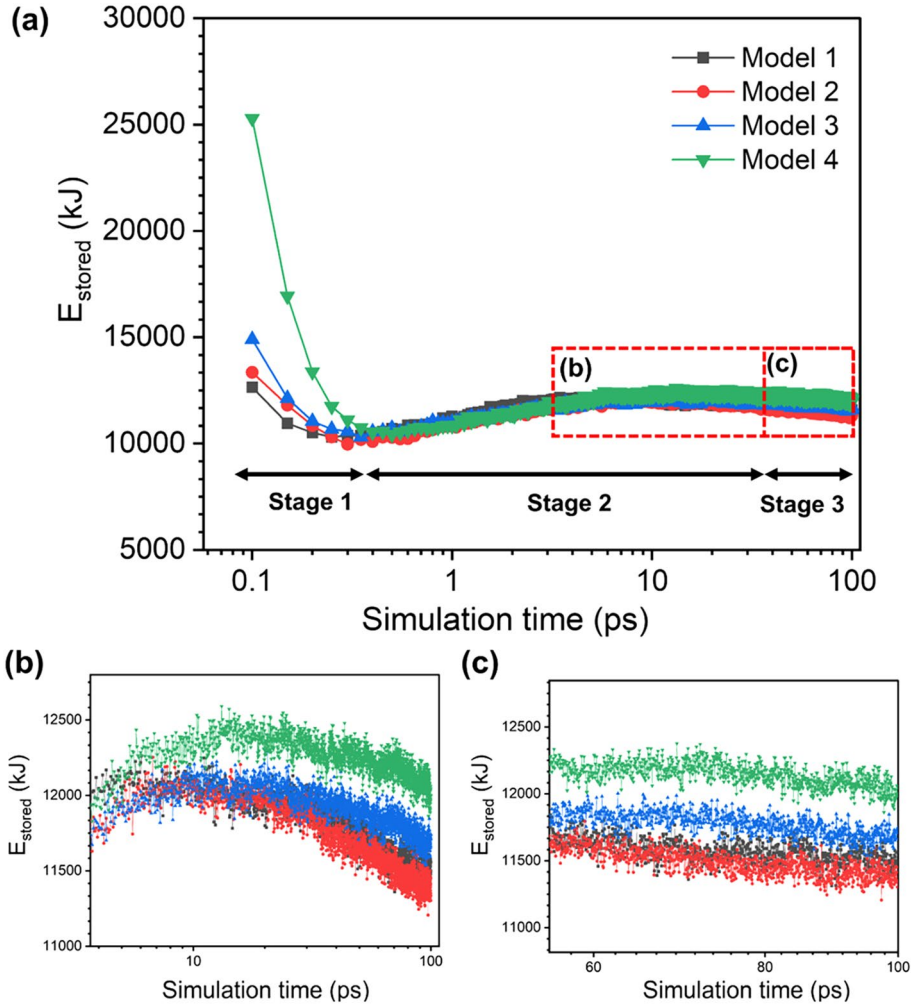

Fig. 2. The stored energy behaviour of simulated MRE models showing (**a**) all stages, (**b**) deformation and (**c**) steady state deformation during stress relaxation phenemonon.

simulation time, the E_{stored} of all MRE models gradually decreases and reaches stable deformation stage (red dotted box (c)), suggesting the completion of the stress relaxation process. It is noticeable that there is insignificant difference for E_{stored} during this steady state deformation, as shown in Fig. 2c, indicating that the internal molecular response of MRE and external strain (0.01%) achieve equilibrium state.

Table 1 shows the stored energy evolution of MRE models over simulation time. An increase in E_{stored} difference ranging from 8.63% to 52.37% is observed in all MRE models. This observation signifies the effect of Fe particles on the stress relaxation phenomenon in MRE, in which greater particles contents induce higher E_{stored} difference. For example, model 3 with 70 wt% Fe particles induces a decrease in E_{stored} of about 21.42% after the simulation. Note there is a systematic discrepancy of the stress relaxation experiment[5] in which the storage modulus of MRE with 70 wt% of CIPs decreased by about 0.5% by the end of the test duration compared to the simulation result. Previous study[29] mentioned that quantitative comparisons between MD simulations and experiments may offer discrepancy due to differences in length and time scales. In this work, the discrepancy is due to the time used during the simulation is within small scale (1×10^{-10} s).

In contrast to the experimental approach, utilizing MD simulation provides an additional quantitative tool for assessing the time-dependent effect of stored energy of MRE model during stress relaxation. In the present study, the important point is decreasing trend of stored energy over time, indicating the occurrence of stress relaxation phenomenon within the LVE region of MRE. Therefore, the MD simulation emerges as a promising computational method and contributes to an understanding of the changes in stored energy in MRE samples during stress relaxation from atomic level.

It is reasonable to expect that the stress relaxation phenomenon in MRE is a consequence of its specific atomic structure. Based on this idea, various forms of energy of MRE models under the stress relaxation are calculated and presented in Fig. 3. Variations of potential energy ($E_{potential}$) of MRE models over increasing simulation time is presented in Fig. 3a. The $E_{potential}$ of a simulated model is a sum of intramolecular potentials (covalent bond) and intermolecular potentials (non-covalent bond). Apparently, the $E_{potential}$ showed a gradual decrease over simulation time. The trend of $E_{potential}$ resembles the trend of E_{stored} (Fig. 2a, suggesting the stress relaxation

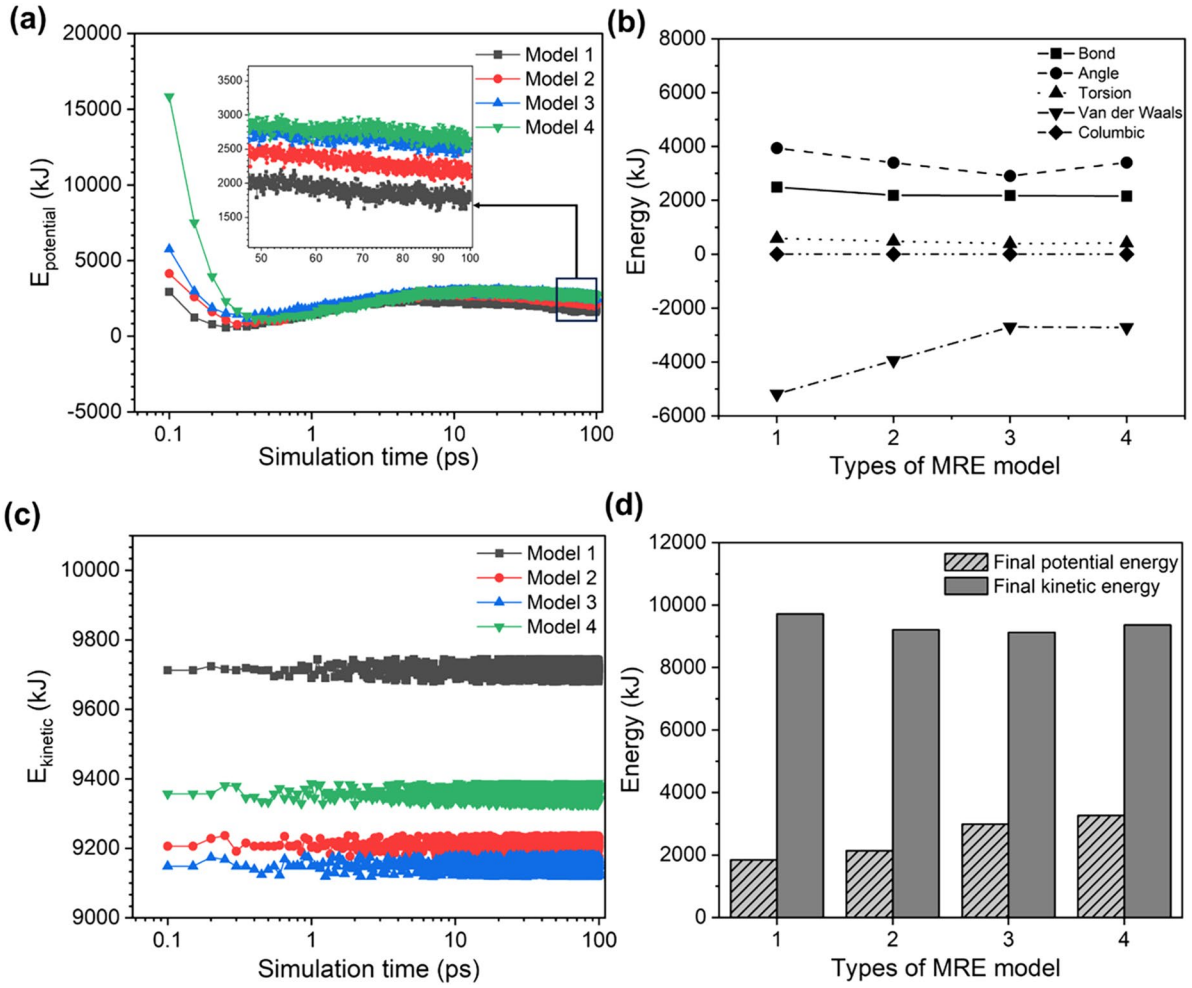

Fig. 3. Changes in (**a**) potential energy, (**b**) covalent and non-covalent bonds energies, (**c**) kinetic energy and (**d**) difference in final potential and kinetic energies in the simulated MRE models with various Fe particles content.

Fe particles contents (wt%)	Initial stored energy (kJ)	Final stored energy (kJ)	Difference (%)
50	12,649	11,557	8.63
60	13,346	11,336	15.06
70	14,899	11,707	21.42
80	25,289	12,045	52.37

Table 1. Stored energy evolution of MRE models with different Fe particles contents.

phenomenon is largely contributed by the change in potential energy of atoms in MRE models. It is also observed that the final in potential energy (final E_{stored}) increased as the Fe particles contents increased, as shown in the inset of Fig. 3a. While the shear deformation of all MRE models occurs after the initial 0.1 ps, it is interesting to observe the higher final $E_{potential}$ (> 2000 kJ) in MRE model 2–4 compared to model 1, suggesting that > 50 wt% of Fe particles causes higher intramolecular and intermolecular potentials.

To further understand, the components of $E_{potential}$ of elements in MRE model such as the covalent bond and non-covalent bond interactions are calculated and presented in Fig. 3b. The covalent bond interaction is composed of energies of bond stretching, angle bending and dihedral torsion between atoms, while the non-covalent bond is the van der Waals and columbic interactions[30,31]. Evidently, covalent bond energy is higher than the non-covalent bond energy in all MRE models, suggesting that the attraction between covalently bonded atoms are much higher than the short range van der Waals forces. The bond energy (2492–2157 kJ) and angle energy (3942–3403 kJ) are higher than torsion energy (590–417 kJ) of atoms in all MRE models because breaking covalent bond require more energy compared to relatively lower energy required for torsional rotation of each bond.

Table 2 shows the values of various energy of MRE models. The highest final $E_{potential}$ (3262 kJ) of MRE model 4 is mainly contributed by the covalent bond interactions that includes the bond (2157 kJ), angle (3403 kJ),

Fe particles (wt%)	Final potential energy (kJ)	Bond energy (kJ)	Angle energy (kJ)	Torsion energy (kJ)	Van der Waals energy (kJ)	Columbic energy (kJ)	Final kinetic energy (kJ)
50	1843.40	2492.40	3942.18	590.18	− 5187.58	6.22	9717.17
60	2142.02	2190.47	3399.48	483.82	− 3937.97	3.37	9206.21
70	2984.97	2179.58	3106.13	394.35	− 2697.02	1.93	9127.31
80	3262.86	2157.61	3403.27	417.12	− 2717.29	2.15	9362.65

Table 2. Energy evolution of MRE models with different Fe particles contents.

torsion (417 kJ) energies compared to weak van der Waals energy (− 2717 kJ) and columbic energy (2 kJ). This explains the slower deformation of E_{stored} model 4, as previously discussed. Furthermore, the change in $E_{potential}$ of the elements in MRE models also is largely affected by the van der Waals energy, as seen increases with increasing Fe particles. The stronger van der Waals energy in MRE model 3 (− 2697 kJ) and model 4 (− 2717 kJ) than model 1 (− 5187 kJ) suggest that there is a strengthening of van der Waals interactions with addition of 70 and 80 wt% of Fe particles.

The increase in van der Waals energy in MRE model 3 signifies an increase in the attractive forces between MRE molecules due to shear-induced changes in molecular proximity. To elaborate further, the shear forces can bring MRE molecules closer together and alter their orientations, leading to increased contact between them. When more Fe particles are present, the enhanced proximity between Fe, SR and VTMS molecules can result in stronger van der Waals energy probably due to greater overlap of electron clouds. Therefore, the stronger van der Waals energy can promote tighter packing of molecules and breaking of the bonds in these MRE models become hard and results in higher onset deformation. This observation is also described in previous study[32] that 80 wt% of CIPs has more tendency to form aggregates than MRE with low CIPs content.

Figure 3c shows the kinetic energy ($E_{kinetic}$) of all MRE models. The $E_{kinetic}$ seems to be consistent over simulation time because the temperature of the system is homologous (T = 25 °C) throughout the entire shear simulation. The almost-consistent $E_{kinetic}$ also indicates the structural stability of MRE models during the stress relaxation phenomenon. Previous study demonstrated that the entanglement of molecular chains in the amorphous system improved the structural stability[33]. An interesting observation is that particles in MRE model 2, 3, and 4 exhibit lower $E_{kinetic}$ than model 1. For instance, MRE model 3 exhibit a lower $E_{kinetic}$ (9127 kJ) compared model 1 (9717 kJ). The decrease of the $E_{kinetic}$ of model 3 by approximately 6% is presumably due to the increased final potential energy (2983 kJ) caused by non-covalent bond interactions of van der Waals energy (− 2697.02) when more Fe particles are introduced. Therefore, the mobility of molecules in MRE models are more restricted and results in low kinetic energy in model with high Fe particles contents.

Variations of final $E_{potential}$ and $E_{kinetic}$ of MRE models with various Fe particles contents are presented in Fig. 3d. The observation is apparent in which the trend of final $E_{potential}$ and $E_{kinetic}$ alternates as the final $E_{potential}$ increases and final $E_{kinetic}$ decreases with an increase in Fe particle contents. This indicates that stronger intramolecular and intermolecular interactions, attributed to higher Fe particles contents and hence, increase the potential energy of MRE model. Consequently, the increased potential energy constrain the movement of MRE particles during stress relaxation phenomenon, and therefore decrease the kinetic energy of particles.

Dynamics behaviour of MRE under stress relaxation through MD simulation

The dynamics analysis of MRE was studied with an aim to elucidate the molecular behaviour of MRE from the atomic level perspective. In MD simulations, the displacement of particles is a fundamental aspect and it involves modelling the motion of particles. Figure 4 presents an illustration of MRE models in 3D simulation space during the stress relaxation. When the simulation time starts at 0 s, it is observable that molecules of Fe, SR and VTMS still adhere to the wall of the simulation boxes. This illustrates the non displacement of particles during the initial simulation time.

By the end of simulation time (t = 100 ps), it is noticeable that the cluster of Fe particles are displaced into largely-separated Fe atoms that move outside the simulation box. The detachment of Fe atoms away from SR molecules in all MRE models, as shown in Fig. 4a–d represents the shearing of Fe particles during the stress relaxation. It is also apparent that the large cluster of SR molecules has been divided into pieces in MRE model with the highest Fe content (80 wt%), indicating that the matrix particles (SR) has been sheared during the stress relaxation. The shearing of the SR matrix prevents energy from being stored, causing it to instead dissipate into the surrounding atoms. This theoretical finding is supported by previous experimental study that discovered the reduction of matrix elasticity as a result to the formation of shear band during the stress relaxation[5]. Therefore, through these illustration, it is interesting to visualise the change in displacement of particles in MRE from the atomistic perspective using the MD simulation.

The radial distribution function (RDF) values shows a specific peak at a distance r in a simulated model. As shown in Fig. 5, there are few peaks present at different distance, the highest peak is located in the range of 1.0–1.1 Å, that represents chemical bonds and hydrogen bonds[14]. It can be observed that Model 4 has the highest intensity compared to other models, as shown in the inset of Fig. 5. This suggests that MRE model 4 with 80 wt% Fe particles exhibit stronger intramolecular and intermolecular bondings than other Fe particles contents.

The mean square displacement (MSD) represents the mobility of molecules from an initial simulation until end of simulation time[34]. MSD also is a measure of average energy particles have moved from their initial positions over a given time interval[14]. Figure 6 shows the MSD curves for all MRE models as a function of simulation

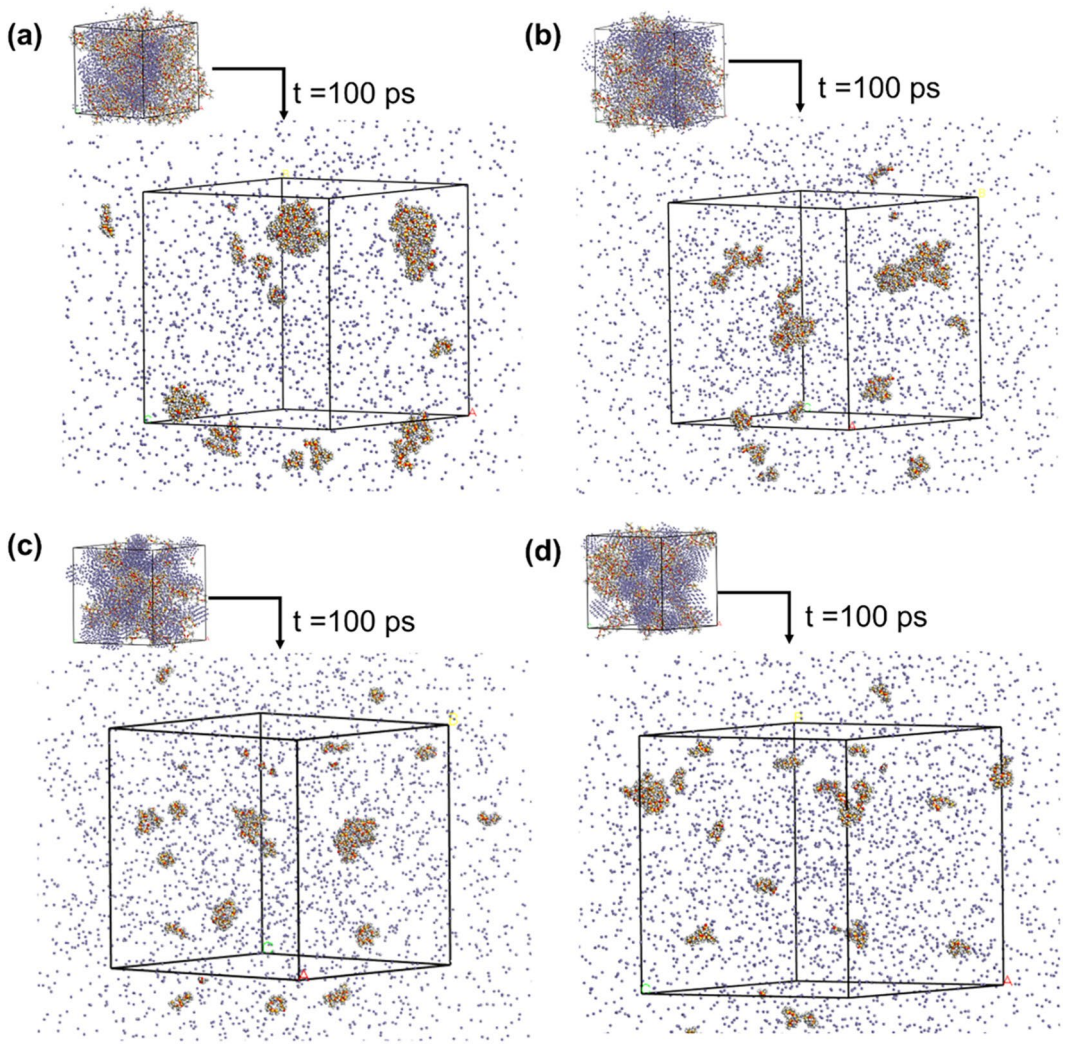

Fig. 4. Illustration of displacement of particles in the MRE models (**a**) 1–50 wt%, (**b**) 2–60 wt%, (**c**) 3–70 wt% and (**d**) 4–80 wt% of Fe particles during the stress relaxation.

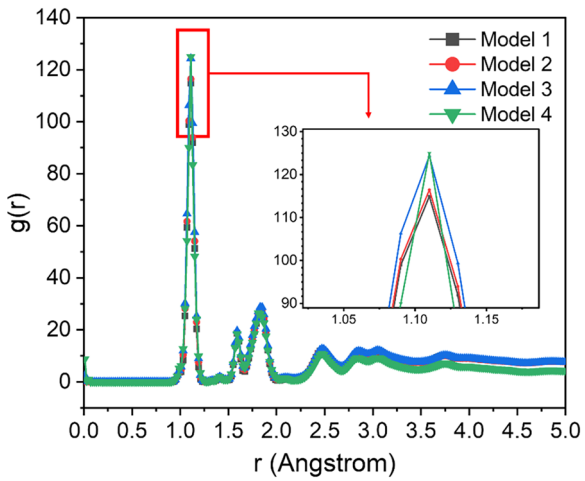

Fig. 5. Radial distribution function values of MRE models.

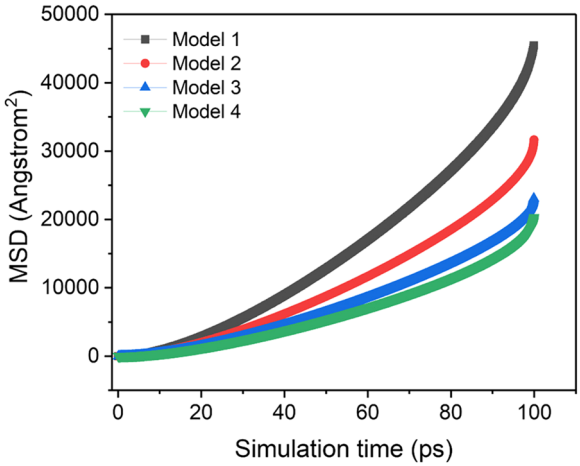

Fig. 6. Mean square displacement curves of MRE models.

time. The MSD values increases with increasing simulation time, indicating the MRE particles are moving when the stress relaxation occurs. Notably, the final MSD value increased with decreasing Fe particles contents. This MSD result is similar with previous study[35] that revealed increasing additive contents to phenyl silicone rubber causes a decrease of mobility of rubber chains.

The MRE model 1 exhibit the highest final MSD value of 45,476 Å at 100 ps, indicating more extensive particle movement over time. This result corroborates with high final kinetic energy of MRE model 1 (9717 kJ). This suggests the MRE model with 50 wt% of Fe particles with higher kinetic energy tend to move freely during stress relaxation. Comparatively, the MSD of MRE model 4 exhibit the lowest final MSD value of 20,318 Å^2. In fact, by the end of simulation time, the final MSD of MRE model 4 decreased about 30% than that model 1.This indicates the addition of 80 wt% of Fe particles results in hindered mobility of MRE chains and MRE particles are not moving much from their initial positions during the shear process. This result also agrees with its low final kinetic energy (9362 kJ). Another previous studies[36,37] mentioned that limited mobility of rubber chains is likely due to the added particles acting as obstacles. In this work, higher Fe particles content hinders the mobility of molecular chains during shear process, and hence, lower MSD values in MRE models.

Experimental

Material and preparation of MREs

Silicone rubber (SR) type RTV-A NS625 in the form of viscous white liquid having density of 1.08 g/cm^3 and viscosity of 18 ± 2 Pa s at 25 °C was supplied by Nippon Steel Corporation, Tokyo, Japan and used as the MRE matrix. The spherical carbonyl iron particles (CIPs) (BASF Corporation, Ludwigshafen, Germany) with the produce code of carbonyl iron powder OM grade (Number 51258195) and an average diameter of 4 µm, was used as magnetic particles. The MRE samples were prepared according to the formulation of 70:30 ratio, in which 70 wt% of CIPs was added to 30 wt% of SR. This ratio is selected based on the previous study[6] that found 70 wt% of CIPs is the optimum content for the improvement in the rheological properties of MREs. The SR and CIPs were homogenously mixed thoroughly using a mechanical stirrer (WiseStir HT-DX, PMI-Labortechnik GmbH, Switzerland) at a stirring speed of 200 rpm for 30 min. Immediately after 30 min, vinyltrimethoxysilane (VTMS) curing agent (Nippon Steel Corporation, Tokyo, Japan) was added into the mixture in 1.5 wt% and stirred rigorously for another 2 min. The resulting mixture was then cast over a rectangular mold and allowed to cure at room temperature for four hours to form a 1 mm thick MRE sheet. The sheet was dried and stored in desiccator prior to testing.

Experimental oscillatory shear rheometry test

For the determination of LVE region, the oscillatory shear rheometry test was performed. The MRE samples were prepared by cutting the MRE sheet into MRE circular samples having diameter of 20 mm and thickness of 1 mm, by using hollow hole punch tool. The storage modulus measurement was performed using an oscillation parallel plate rheometer (MCR 302 Anton Paar, Austria). The temperature control device (Viscotherm VT2, Anton Paar, Austria) was utilized for controlling the measuring temperature to be at 25 °C. The parallel plate (PP20) was suitably selected according to the dimension of the MRE samples (20 mm diameter). The MRE sample was centrally placed between the top rotary and bottom parallel plates of the rheometer. In this study, an oscillatory shear rheometry test mode under constant frequency (1 Hz) was used for entire experiment. The strain amplitude sweep was performed in order to measure the storage modulus that is proportionate to the stored energy within viscoelastic materials during the oscillatory shear rheometer. For the strain amplitude sweep, the shear strain was increased continuously from 0.001 to 10% throughout the test with an interval of 30 points and the total duration of the test was set to 150 s. The oscillatory shear rheometer was repeated for three times to get an average result.

Model and simulation details

The MD simulation was performed using Dassault Systemes BIOVIA Materials Studio software. Generally, the MD simulation comprises of three stages which are the construction of model, equilibration, and production steps. For the first step (construction of model), the silicone rubber (SR), magnetic iron (Fe) particles and vinyltrimethoxysilane (VTMS) molecules were modelled using the Materials Visualizer within the software. The SR, Fe particles and VTMS molecules were built based on their chemical structures. All molecules underwent the geometry optimization process. Having modelled all the molecules, the final step in constructing a model for subsequent simulation is defining the periodic simulation box. For this purpose, the Fe particles and VTMS molecules were randomly distributed in the SR system, according to weight percentage (wt%), as listed in Table 3. Figure 7 presents the three-dimensional (3D) simulation box that represents the MRE models with 50, 60, 70, and 80 wt% of Fe particles, that labelled as model 1, 2, 3, and 4, respectively. The size of magnetic iron particles in MD simulation is about 10 nm. All models were constructed using the Amorphous Cell construction module. The simulation box dimensions for the MRE models were set as $35.3 \times 35.3 \times 35.3$ Å^3.

After model construction, an equilibration step involving an energy minimization module was performed to equilibrate this molecular system. For this step, the MRE model was integrated under the NVT canonical ensemble at 25 °C to let the molecules to relax and achieve a zero initial stress state at this particular temperature. The energy convergence threshold was set to minimum energy of 0.001 kcal/mol, and total simulation steps of 100,000 with the time step of 1 femtosecond (fs) were employed. A short time step (1 fs) is required to ensure numerical stability. The final MRE model was used for subsequent molecular simulation.

The production step, which is the shear simulation, was performed using the Forcite shear module. Figure 8 shows the flowchart of approach taken for the shear simulation method. In general, the shear simulation mimics the experiment in which the material is placed between two plates and then sheared according to the choice of the shear direction. The velocity profile of the molecular system can be generated by sliding the upper and lower walls in either left and right directions[38]. Some key parameters of the module were determined before the simulation. In this work, the choice of NPT ensemble was selected because this ensemble can conserve constant particles at a constant temperature. The forcefield energy was set to universal, with the charges of the molecules were set to current. Moreover, the timestep of 1 fs was selected and total simulation steps was set to 100,000 during the simulation to ensure accurate data are obtained. The frame output was obtained every 100 steps during simulation. Furthermore, the Ewald summation method was used for calculating electrostatic interaction with accuracy level of 0.001 kcal/mol with the buffer width of 0.5 Å. The atom-based summation method for Van der Waals forces with the truncation method of cubic spline with the buffer width of 0.5 Å were selected. Other key parameters such as the shear strain of 0.01% and simulation temperature of 25 °C, were fixed throughout the entire shear simulation. Following the shear simulation setup, the MRE model was selected as the input. The shear simulation was performed on each model according to the fixed setup. The shear direction (plane) was specified to be at plane B (top) of the simulation cell to mimic the movement of the top rotary plate of the rheometer. In the rheology of viscoelastic materials, the stored energy during deformation is proportional to the shear storage modulus, that can be expressed as the following Eq. (1)[39,40]:

$$E_s = \frac{G'\gamma_o^2}{2} \tag{1}$$

where E_s is the stored energy, G′ is the shear storage modulus and γ_o is the strain amplitude.

The stored energy of the MRE model was calculated as the sum of potential and kinetic energies (i.e., the SR matrix phase and Fe particles phase) as shown in Eq. (2):

$$E_{\text{stored}} = E_{\text{potential}} + E_{\text{kinetic}} \tag{2}$$

where E_{stored} represents the stored energy that is equivalent to total energy, $E_{\text{potential}}$ and E_{kinetic} represent the potential energy and kinetic energy of the simulated MRE system, respectively.

The potential energy of the MRE model was calculated as the sum of intramolecular and intermolecular potentials, as shown in Eq. (3):

$$E_{\text{potential}} = E_{\text{bond}} + E_{\text{angle}} + E_{\text{torsion}} + E_{\text{van der Waals}} + E_{\text{columbic}} \tag{3}$$

where E_{bond}, E_{angle}, E_{torsion}, represents the intramolecular potentials which are the bond energy, angle energy, torsion energy, respectively. The intermolecular potentials are represented by the van der Waals energy ($E_{\text{van der Waals}}$) and columbic energy (E_{columbic}) of the simulated MRE models.

The kinetic energy of the MRE model was calculated using the classical mechanics formula as shown in Eq. (4):

Silicone rubber (wt%)	Fe particles (wt%)	VTMS (wt%)	MRE model
50	50	1.5	1
40	60	1.5	2
30	70	1.5	3
20	80	1.5	4

Table 3. Model naming convention used for MD simulation.

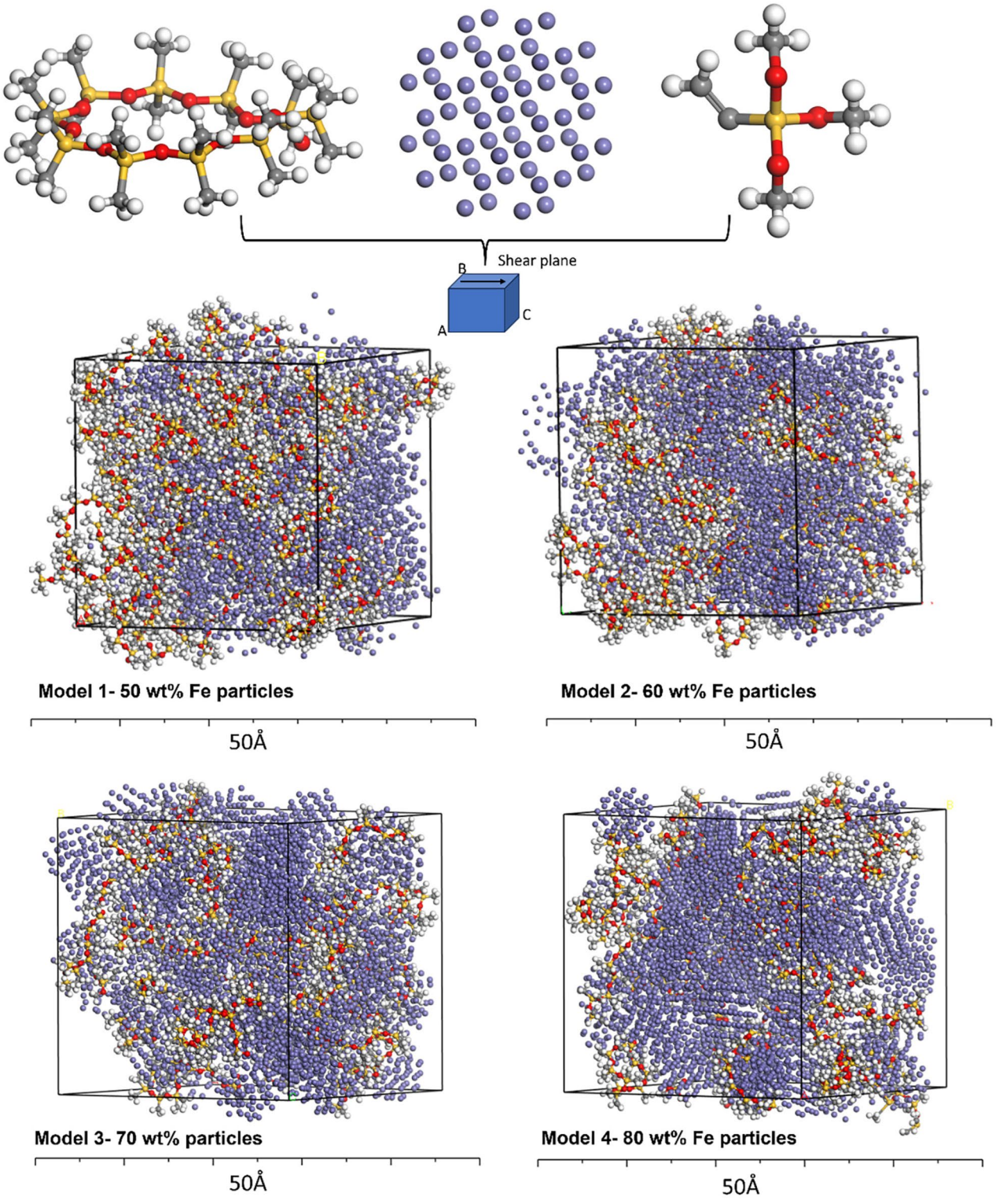

Fig. 7. Models for MD simulation of MREs (grey, red, white, purple and yellow spheres represent C, O, H, Fe and Si atoms, respectively).

$$E_{\text{kinetic}} = \frac{1}{2}\sum_{i=1}^{N} m_i v_i^2 \tag{4}$$

where N is the total number of particles, m_i is the mass of the i-th particle, v_i is the velocity vector of the i-th particle.

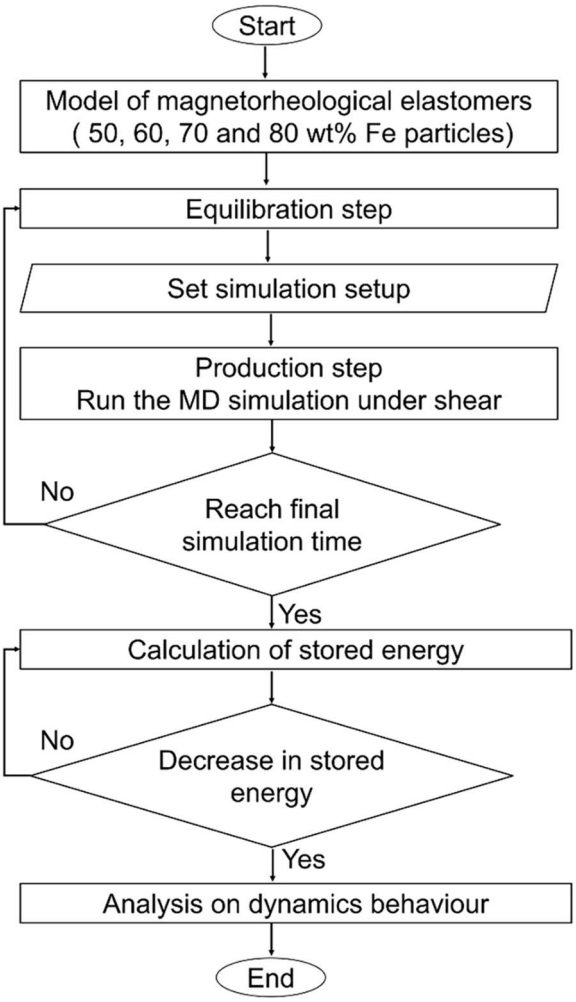

Fig. 8. Overall flowchart of the MD simulation method in characterizing energy and dynamics behaviour of MRE models.

After running simulation under the shear deformation mode, if the simulation results show the stress relaxation phenomenon, which is in this study, the gradual decrease of stored energy over simulation time, the dynamics of the simulated model was then characterized using the Forcite Analysis module. The determination of mean square displacement (MSD) values of the simulated model was calculated according to the trajectory results after simulation by using Eq. (5):

$$MSD = \left| r(t)^2 - r(0)^2 \right| \tag{5}$$

where r(t) and $r(0)$ represent position of the mass center for the molecule at time t and 0, respectively.

Another information obtained from the dynamics analysis is the radial distribution function (RDF), which is a tool to characterize the molecular structure that evaluates the relative probability of finding a particle at a distance r from the reference position (g(r)).

Conclusion

In this investigation, the MD simulation was employed to investigate energy and dynamics behavior of MRE during stress relaxation. The experimental shear rheometer showed that the linear viscoelastic region of MRE with 70 wt% CIPs is within 0.001–0.01% of strain. Furthermore, the stored energy of all MRE models MRE models containing 50–80 wt% of Fe particles decreased over time, demonstrating that the stress relaxation can still occur within the LVE region of MRE. During stress relaxation, the potential energy of particles in all MRE models decreased over time, due to the change in covalent bond interactions, van der Waals and Columbic interactions. Notably, the high final E_{stored} in the MRE model with 80 wt% of Fe particles is due to the increased intramolecular and intermolecular interactions. Furthermore, the mobility of this MRE model also decreased, as shown by the lowest final MSD value (20,318 Å^2). The results indicate that MD simulation proves to be a promising quantitative tool for comprehending the alterations in energy and dynamics behavior exhibited by

MRE during stress relaxation. This study is advantageous for examining stress relaxation from an atomic level perspective and for advancing the development of MRE in the field of nanotechnology.

Data availability

The datasets used and/or analysed during the current study available from the corresponding author on reasonable request.

Received: 20 May 2024; Accepted: 16 August 2024
Published online: 25 August 2024

References

1. Fakhree, M. A. M. *et al.* Field-dependent rheological properties of magnetorheological elastomer with fountain-like particle chain alignment. *Micromachines* **13**, 492 (2022).
2. Loukil, M. T. *et al.* Stored energy accompanying cyclic deformation of filled rubber. *Eur. Polym. J.* **98**, 448–455 (2018).
3. Hosseini, S. M., Shojaeefard, M. H. & Saeidi Googarchin, H. Fatigue life prediction of magneto-rheological elastomers in magnetic field. *Mater. Res. Express* **8**, 025304 (2021).
4. Johari, M. A. F. *et al.* Microstructural behavior of magnetorheological elastomer undergoing durability evaluation by stress relaxation. *Sci. Rep.* **11**, 1–17 (2021).
5. Johari, M. A. F. *et al.* Shear band formation in magnetorheological elastomer under stress relaxation. *Smart Mater. Struct.* **30**, 045015 (2021).
6. Johari, M. A. F. *et al.* Microstructural behavior of magnetorheological elastomer undergoing durability evaluation by stress relaxation. *Sci. Rep.* **11**, 10936 (2021).
7. Becker, T. I., Zimmermann, K., Borin, D. Y., Stepanov, G. V. & Storozhenko, P. A. Dynamic response of a sensor element made of magnetic hybrid elastomer with controllable properties. *J. Magn. Magn. Mater.* **449**, 77–82 (2018).
8. Nam, T. H., Petríková, I. & Marvalová, B. Stress relaxation behavior of isotropic and anisotropic magnetorheological elastomers. *Contin. Mech. Thermodyn.* **36**, 299–315 (2024).
9. Nam, T. H., Petríková, I. & Marvalová, B. Experimental and numerical research of stress relaxation behavior of magnetorheological elastomer. *Polym. Test.* **93**, 106886 (2021).
10. Zhang, H., Zhou, Z., Qiu, J., Chen, P. & Sun, W. Defect engineering of carbon nanotubes and its effect on mechanical properties of carbon nanotubes/polymer nanocomposites: A molecular dynamics study. *Compos. Commun.* **28**, 100911 (2021).
11. Zhou, X. Y., Wu, H. H., Zhu, J. H., Li, B. & Wu, Y. Plastic deformation mechanism in crystal-glass high entropy alloy composites studied via molecular dynamics simulations. *Compos. Commun.* **24**, 100658 (2021).
12. Guo, Y. *et al.* A combined molecular dynamics simulation and experimental method to study the compatibility between elastomers and resins. *RSC Adv.* **8**, 14401–14413 (2018).
13. Izadi, R., Tuna, M., Trovalusci, P. & Fantuzzi, N. Thermomechanical characteristics of green nanofibers made from polylactic acid: An insight into tensile behavior via molecular dynamics simulation. *Mech. Mater.* **181**, 104640 (2023).
14. Cai, H. *et al.* Experimental and computational investigation on performances of the thermoplastic elastomer SEBS/Poly(lactic acid) blends. *Mater. Today Commun.* **35**, 105600 (2023).
15. Ryu, M. S. *et al.* Prediction of the glass transition temperature and design of phase diagrams of butadiene rubber and styrene–butadiene rubber via molecular dynamics simulations. *Phys. Chem. Chem. Phys.* **19**, 16498–16506 (2017).
16. Zhao, W., Xiao, R., Steinmann, P. & Pfaller, S. Time–temperature correlations of amorphous thermoplastics at large strains based on molecular dynamics simulations. *Mech. Mater.* **190**, 104926 (2024).
17. Gao, X. The mathematics of the ensemble theory. *Results Phys.* **34**, 105230 (2022).
18. Zhang, Z. *et al.* Quantitatively predicting the mechanical behavior of elastomers via fully atomistic molecular dynamics simulation. *Polymer* **223**, 123704 (2021).
19. Ji, K., Stewart, L. K. & Arson, C. Molecular dynamics analysis of silica/PMMA interface shear behavior. *Polymers* **14**, 1039 (2022).
20. Jeong, S. & Baig, C. Molecular process of stress relaxation for sheared polymer melts. *Polymer* **202**, 122683 (2020).
21. Tamir, E., Srebnik, S. & Sidess, A. Prediction of the relaxation modulus of a fluoroelastomer using molecular dynamics simulation. *Chem. Eng. Sci.* **225**, 115786 (2020).
22. Johari, M. A. F. *et al.* The effect of microparticles on the storage modulus and durability behavior of magnetorheological elastomer. *Micromachines* **12**, 948 (2021).
23. Leng, D. X. *et al.* Experimental mechanics and numerical prediction on stress relaxation and unrecoverable damage characteristics of rubber materials. *Polym. Test.* **98**, 107183 (2021).
24. Lin, C. Y., Chen, Y. C., Lin, C. H. & Chang, K. V. Constitutive equations for analyzing stress relaxation and creep of viscoelastic materials based on standard linear solid model derived with finite loading rate. *Polymers* **14**, 2124 (2022).
25. Tobolsky, A. V., Prettyman, I. B. & Dillon, J. H. Stress relaxation of natural and synthetic rubber stocks. *Rubber Chem. Technol.* **17**, 551–575 (1944).
26. Liu, A., Lin, W. & Jiang, J. Investigation of the long-term strength properties of a discontinuity by shear relaxation tests. *Rock Mech. Rock Eng.* **53**, 831–840 (2020).
27. Meera, A. P., Said, S., Grohens, Y., Luyt, A. S. & Thomas, S. Tensile stress relaxation studies of TiO2 and nanosilica filled natural rubber composites. *Ind. Eng. Chem. Res.* **48**, 3410–3416 (2009).
28. Ahmad Khairi, M. H. *et al.* Role of additives in enhancing the rheological properties of magnetorheological solids: A review. *Adv. Eng. Mater.* **21**, 1800696 (2019).
29. Tian, X. *et al.* Anisotropic shock responses of nanoporous Al by molecular dynamics simulations. *PLoS ONE* **16**, e0247172 (2021).
30. Li, S. *et al.* All-atom molecular dynamics simulation of structure, dynamics and mechanics of elastomeric polymer materials in a wide range of pressure and temperature. *Mol. Syst. Des. Eng.* **9**, 264–277 (2024).
31. Saha, S. & Bhowmick, A. K. Computer aided simulation of thermoplastic elastomer from poly (vinylidene fluoride)/hydrogenated nitrile rubber blend and its experimental verification. *Polymer* **112**, 402–413 (2017).
32. Salem, A. M. H., Ali, A., Ramli, R., Bin, M. A. G. A. & Julai, S. Effect of carbonyl iron particle types on the structure and performance of magnetorheological elastomers: A frequency and strain dependent study. *Polymers* **14**, 4193 (2022).
33. Qi, S., Yu, M., Fu, J. & Zhu, M. Stress relaxation behavior of magnetorheological elastomer: Experimental and modeling study. *J. Intell. Mater. Syst. Struct.* **29**, 205–213 (2018).
34. Paul, S. K. *et al.* Molecular modeling, molecular dynamics simulation, and essential dynamics analysis of grancalcin: An upregulated biomarker in experimental autoimmune encephalomyelitis mice. *Heliyon* **8**, 11232 (2022).
35. Zhu, L. *et al.* Tetraphenylphenyl-modified damping additives for silicone rubber: Experimental and molecular simulation investigation. *Mater. Des.* **202**, 109551 (2021).
36. Shi, R. *et al.* Tensile performance and viscoelastic properties of rubber nanocomposites filled with silica nanoparticles: A molecular dynamics simulation study. *Chem. Eng. Sci.* **267**, 118318 (2023).

37. Mohamad, N. *et al.* A comparative work on the magnetic field-dependent properties of plate-like and spherical iron particle-based magnetorheological grease. *PLoS ONE* **13**, e0191795 (2018).
38. Sharma, S., Kumar, P. & Chandra, R. Introduction to Molecular Dynamics. In *Molecular Dynamics Simulation of Nanocomposites Using BIOVIA Materials Studio, Lammps and Gromacs* 1–38 (Elsevier, 2019).
39. Tschoegl, N. W. *The Phenomenological Theory of Linear Viscoelastic Behavior. The Phenomenological Theory of Linear Viscoelastic Behavior* (Springer, 1989).
40. Mezger, T. *The Rheology Handbook* (Vincentz Network, 2020).

Acknowledgements

The authors acknowledge the financial support provided by UTM Fundamental Research (Vot No. 22H14) and Professional Development Research University (PDRU) (Vot. No. 06E95). Author M.S. wishes to thank the Czech Science Foundation [23-07244S] for the financial support.

Author contributions

N.H.L. conducted the experiments and simulations, analysed the data, prepared the figures and wrote the main manuscript, while S.A.M. and M.S. supervised the entire practical work and reviewed the manuscript. M.A.F.J., N.A.N., and S.M.Y. reviewed the manuscript.

Competing interests

The authors declare no competing interests.

Additional information

Correspondence and requests for materials should be addressed to S.A.M. or M.S.

Reprints and permissions information is available at www.nature.com/reprints.

Publisher's note Springer Nature remains neutral with regard to jurisdictional claims in published maps and institutional affiliations.